

Marker location and knee joint constraint affect the reporting of overhead squat kinematics in elite youth football players.

Authors

Lara M. Coyne ^{a,df}, Micheál Newell ^a, Marco J.M. Hoozemans ^b, Andrew Morrison ^c, Susan J. Brown^e.

a School of Medicine, National University of Ireland, Galway, Ireland.

b Department of Human Movement Sciences, Faculty of Behavioural and Movement Sciences, Vrije Universiteit Amsterdam, Amsterdam Movement Sciences, Amsterdam, The Netherlands.

c Cambridge Centre for Sports and Exercise Sciences, Anglia Ruskin University, Cambridge, U.K.

d Arsenal Performance & Research Team, Arsenal Football Club, London, UK

e Edinburgh Napier University, School of Applied Sciences Edinburgh, Scotland.

f Insight, Centre for Data Analytics, National University of Ireland, Galway, Ireland.

*Correspondence: Su.Brown@napier.ac.uk

Marker location and knee joint constraint affect the reporting of overhead squat kinematics in elite youth football players.

Abstract

Motion capture systems are used in the analysis and interpretation of athlete movement patterns for a variety of reasons, but data integrity remains critical regardless of the purpose of measurement. The extent to which marker location or constraining degrees of freedom in the biomechanical model impacts on this integrity lacks consensus. Elite youth academy footballers (n=10) performed repeated bilateral overhead squats using a marker-based motion capture system. Kinematic data were calculated using four different marker sets with three degrees of freedom (3DOF) and six degrees of freedom (6DOF) configurations for the three joint rotations of the right knee. Root mean squared error (RMSE) differences between marker sets ranged in the sagittal plane between 1.02 and 4.19 degrees to larger values in the frontal (1.30- 6.39 degrees) and transverse planes (1.33 and 7.97 degrees). The cross-correlation function (CCF) of the knee kinematic time series for all eight marker-sets ranged from excellent for sagittal plane motion (>0.99) but reduced for both coronal and transverse planes (< 0.9). Two-way ANOVA repeated measures for marker sets calculated for all directions at peak squat knee flexion revealed significant differences between marker sets for frontal and transverse planes ($p<0.05$). Pairwise transverse plane 6DOF marker set comparisons showed significant differences except between the anterior partial cluster and cluster marker sets. The paired 3DOF comparison revealed a significant difference between two of the four marker sets. The 3DOF and 6DOF model comparisons demonstrated significant differences except for the anterior partial cluster. Marker location and constraining DOF while measuring relatively large ranges of motion in this population are important considerations for data integrity. This was particularly evident in the measurement of frontal and transverse kinematics with implications for future studies using motion capture with athletic populations.

Keywords;

Marker-based motion capture, marker location, overhead squat, constrained, unconstrained kinematic model, knee kinematics, elite youth football

Introduction:

The assessment of injury risk is a key strategy for professional football teams in an attempt to reduce injury occurrence in their players (McCall et al., 2015; McCall, Lewin, O'Driscoll, Witvrouw, & Ardern, 2017). Furthermore, improving movement quality of footballer players has been reported as important for reducing injury risk within this population (Bagwell, Snibbe, Gerhardt, & Powers, 2016; Smale, Potvin, Shourijeh, & Benoit, 2017). The ability to accurately assess movement quality can support athletic development programmes (Bergeron et al., 2015; Bishop, Edwards, & Turner, 2016; Marques, Medeiros, de Souza Stigger, Nakamura, & Baroni, 2017; McCall et al., 2017; Scibek, Moran, & Edmond, 2020) and improve return to play protocols when an injury occurs (Arderon et al., 2018; Leporace et al., 2013; Whittaker et al., 2018). A commonly evaluated movement pattern used within practice and investigative studies is the bilateral overhead squat which encompasses a large range of knee flexion (Bishop, Edwards, et al., 2016; Donohue et al., 2015; Schoenfeld, 2010). Commonly, this assessment of movement quality relies on the experience of relevant practitioners and can be somewhat subjective, or reliant on the ability to make a judgment based on less reliable criterion (Onate et al.,

2012). Therefore, the use of motion capture systems could enhance movement analysis and provide practitioners with more reliable quantitative data for use in subsequent athlete development programmes, rather than qualitatively ranking and rating motion as is the current practice in football.

However, despite reported sub-millimetre accuracy, marker-based motion capture systems are subject to the limitation of soft tissue artefact and muscle contraction that affect the resultant knee kinematics (Fiorentino et al., 2017; Schulz & Kimmel, 2010). Soft tissue artefact (STA), being site, participant and movement task-specific, will impact upon the selection of marker locations and the subsequent biomechanical model utilised (Benoit et al., 2006; Cockcroft, Louw, & Baker, 2016; McFadden, Daniels, & Strike, 2020; Schulz & Kimmel, 2010). The use of bone pins or advanced imaging validation methods to optimise kinematic data (Fiorentino et al., 2017; Mentiplay & Clark, 2018; Potvin, Shourijeh, Smale, & Benoit, 2017) is impractical in sports settings. While there is evidence of the impact of marker location and biomechanical model building within literature (Cockcroft et al., 2016; Mentiplay & Clark, 2018; Robinson, Donnelly, Tsao, & Vanrenterghem, 2013; Slater, Hullfish, & Baxter, 2018) to our knowledge the consideration of best practice in the selection of marker location and model configuration for assessment of the overhead squat has not yet been investigated in professional footballers. Furthermore, previous research on lower limb kinematics and injury risk reduction often lack detail on both marker set and model configuration. Previously reported and validated marker locations include the Conventional Gait Model [CGM] and variations; the Plug-in-Gait model; Helen Hayes marker sets (Baker, Leboeuf, Reay, & Sangeux, 2017; Duffell, Hope, & McGregor, 2014; Schulz & Kimmel, 2010); Cluster-based model (Mentiplay & Clark, 2018) and 6DOF gait models (Buczek, Rainbow, Cooney, Walker, & Sanders, 2010; Collins, Ghoussayni, Ewins, & Kent, 2009; Schmitz et al., 2016; Żuk & Pezowicz, 2015). However, marker locations used in clinical gait analysis are often not validated for other movement patterns (Mentiplay & Clark, 2018; Schulz & Kimmel, 2010).

Attempts to improve the fidelity of segment and segmental interaction data, particularly for the lower limbs include the use of rigid cluster marker sets placed on the thigh and shank (Buczek et al., 2010; Collins et al., 2009; Schache, Baker, & Lamoereux, 2008) and constraining the degrees of freedom within the model for anatomical joints in an attempt to reduce the influence of STA (Duprey, Cheze, & Dumas, 2010; Gasparutto, Sancisi, Jacquelin, Parenti-Castelli, & Dumas, 2015; Potvin et al., 2017; Richard, Cappozzo, & Dumas, 2017). However, there remains some ambiguity around the influence of these decisions on data reliability which may be in part attributable to the nature of the study participants and the type of movement patterns under scrutiny. Additionally, while some marker location and DOF decisions have been reported as reliable in sagittal and frontal plane rotations (Slater et al., 2018), others reported agreement only in the sagittal plane, with no improvement in data reliability when rigid clusters of markers were used (Mantovani & Lamontagne, 2017; Schulz & Kimmel, 2010). In addition, constraining the knee joint to 3DOF has been previously reported not to influence the accuracy of the kinematic outcomes and was reported to have contributed to increased error (Andersen, Benoit, Damsgaard, Ramsey, & Rasmussen, 2010; Fiorentino et al., 2017; Mentiplay & Clark, 2018; Potvin et al., 2017; Richard et al., 2017; Wen et al., 2018). In contrast, marker set test retest reliability of 3DOF and 6DOF models was deemed good to excellent for all except the transverse plane motion, with slightly higher agreement of the 6DOF marker set models reported (Mentiplay & Clark, 2018).

In practice, the ability to accurately report normative 6DOF knee kinematics that includes joint translation is important within professional football, but a challenge for motion capture systems (Lu & O' Connor, 1999; Mentiplay & Clark, 2018; Ojeda, Martínez-Reina, & Mayo, 2014; Richard et al., 2017; Smale et al., 2017). This joint translation may be important to quantify in developing athletic

populations who may present with underlying hypermobility influenced by growth rates and maturation stage resulting in an increased risk of injury (Ryan, Lewin, Forsythe, & McCall, 2018; Smale et al., 2017). These inconsistencies within the literature regarding appropriate marker locations and model constraints, particularly when measuring large-amplitude athletic movement tasks prompted this study. The purpose of this study was to compare knee joint kinematics derived using four different lower limb marker sets and two degrees of freedom models (6DOF and 3DOF), while tracking the overhead squat in an elite youth football population. The null hypothesis was that there would be no difference between the eight configurations in the determination of knee kinematics during the overhead squat.

Methods

Ethics approval was obtained from the National University of Ireland, Galway, Medical Ethics Committee and individual informed consent gained from each participant before testing. All participants were informed of the purpose of testing and advised that they could withdraw at any stage. All data was stored in accordance with GDPR guidelines, including ensuring anonymity of all participants.

Participants

Ten Academy Elite football players (n=10) of mean age (SD): 18.5 (± 1.3) years, height 1.83 (± 0.04) metres and weight 79.2 (± 6.2) kg, volunteered to participate in this study. All participants self-reported their right leg as their dominant kicking leg. Participants wore tight-fitting clothing to reduce extraneous marker movement and the same footwear to standardise testing protocols.

Inclusion criteria

All participants were physically able to perform the overhead squat motion without any restriction. Participants were full-time Premier League academy football players for a minimum of two years and were engaged in supervised strength training. All participants had achieved full maturation status or 100% of Peak Adult Height at the time of testing (Khamis & Roche, 1994; Malina, Rogol, & Cumming, 2015).

Exclusion criteria

Participants were excluded if they reported any musculoskeletal injury or illness that hindered participation in full training or games within the preceding 3 months.

Overhead squat

All participants were instructed using the same verbal and visual demonstration of the overhead squat. Participants were requested to stand with their feet shoulder-width apart, holding a 120-cm wooden dowel pressed overhead with extended arms at the initiation of the trial and then to asked to complete the squat to maximum depth with good trunk control (Bishop, Edwards, et al., 2016). The squat depth was self-determined by participants as per standardised functional movement assessment protocols (Cook, Burton, & Hoogenboom, 2006; Scibek et al., 2020). Motion timing was controlled to two seconds down, and two seconds to return to the start position (Bishop, Villiere, & Turner, 2016). All participants familiarised themselves with the movement prior to data collection under the supervision of a Chartered Physiotherapist.

[Figure 2]

Data collection

Kinematic data were collected using eight infrared cameras (Miquis, Qualisys Medical Ltd., Sweden) operating at 100 Hz surrounding the capture space; a dedicated area adjacent to the strength and conditioning facility of the Academy. The capture volume was calibrated according to the manufacturers' instructions with the camera system showing a maximum calibration residual of 1mm for each camera.

Qualisys Track Manager TM (QTM, Version 2.16 Qualisys Medical Ltd., Sweden) was used to reconstruct the three-dimensional coordinates of each of the 19 mm spherical reflective markers placed on the following sites: right and left Anterior Superior Iliac Spine (ASIS), right and left posterior superior iliac spine (PSIS) right and left medial and lateral femoral condyles, right and left medial malleoli ankle and right and left lateral malleoli ankle. Rigid clusters were placed on the right and left lateral thighs and shanks. The markers on the lateral thigh and shank consisted of a rigid plate (131 x 80 mm) consisting of four markers with the top two markers width 7 cm apart and lengthwise 9 cm (Figure 1 b). The rigid plate was attached with adhesive tape and velcro strapping to the lateral thigh approximately midway between the greater trochanter and the lateral knee markers. Markers were placed on all participants by the same musculoskeletal physiotherapist with over 20 years of experience, under the guidance of a biomechanist with over 15 years of motion capture experience. All reflective markers were visible in all three repetitions of the movement to ensure concurrent data collection. A static trial was collected in the anatomical position for subsequent segment definitions before completing the four overhead squat movement trials.

Data Processing

Kinematic models for each participant were created using Visual 3DTM (version 6.01.16, C-motion, Germantown, MD, USA) as follows:

Segmental and joint centre definitions:

Using the right-hand orthogonal rule, the segment coordinate system (SCS) axes were aligned with the (X) positive axis in the mediolateral direction, positive (Y) axis in the anterior/posterior direction and positive (Z) axis in the vertical direction (Figure 1a). The hip and knee joint centres were determined using a functional joint methods approach and individualised for all participants (Schwartz & Rozumalski, 2005). The squat motion served as the calibration method for the determination of segmental interaction to define the mediolateral knee joint axis (Philp, Leboeuf, Pandyan, & Stewart, 2019), and the hip joint centre. The longitudinal axis of the femur was defined as the line between the functional hip joint centre and the midpoint between the medial and lateral femoral condyle markers projected onto the functional knee axis. All eight marker set model configurations used the same functional hip centres and functional knee axes to define segment interaction according to (Schwartz & Rozumalski, 2005). The shank and pelvis segments were tracked in the same way throughout the overhead squat. Thus, the primary difference between the eight models was how they track the segments articulating at the knee joint. A Cardan rotational sequence of X, Y, Z (Lees, Asai, Andersen, Nunome, & Stetzing, 2010) was applied to the model.

Segment Tracking

Eight different segment reconstructions were created in Visual 3DTM using the 4 marker location sets and two joint constraint methods, 3DOF and 6DOF. For the 3DOF models, DOF was constrained to the three rotations only.

1. **Anatomical (Ana3DOF, Ana6DOF)**: this model used the functional hip joint centre and the medial and lateral knee markers to track the thigh (Schulz & Kimmel, 2010; Slater et al., 2018).
2. **Anterior Partial Cluster Knee (Ant3DOF, Ant6DOF)**: this model used two anterior thigh cluster markers and the medial and lateral knee markers to track the thigh.
3. **Cluster (Clust3DOF, Clust6DOF)**: all four markers on the rigid thigh cluster marker was used to track the thigh (Mentiplay & Clark, 2018; Schulz & Kimmel, 2010).
4. **Posterior Partial Cluster Knee (Post3DOF, Post6DOF)**: this model used the two posterior thigh cluster markers and the medial and lateral knee markers to track the thigh.

[Insert Figure 1 a & b]

For the purpose of data extraction, the start of the overhead squat was defined as the instant when the pelvis vertical downward velocity reached a threshold of $0.1 \text{ m}\cdot\text{s}^{-1}$, and the end at the instant the participant returned to the original upright stance position. The data was time normalised to 101 data points between these two events. A 4th order low-pass Butterworth filter of 7Hz was applied to the data (Cortes et al., 2014).

Data analysis:

The time series of all three knee joint rotations during the overhead squat was evaluated for each marker and DOF configuration. The post-processed knee joint kinematics were examined using summary statistics, and the kinematic difference analysed. The range of differences in measurement between all eight models was expected to fall between 3 to 5 degrees (McGinley, Baker, Wolfe, & Morris, 2009; Slater et al., 2018).

Root mean squared error (RMSE) was used to determine the kinematic differences between all marker sets and model configurations over the whole time series. RMSE values within a five-degree kinematic threshold were considered of 'high fidelity' (Slater et al., 2018). Cross-Correlation Function (Baxter, Sturnick, Demetracopoulos, Ellis, & Deland, 2016) compared the kinematic agreement between all marker set and model combinations over the time series. A correlation of less than 0.9 was deemed substantially different (Slater et al., 2018). RMSE and cross-correlation values were calculated using R (R CoreTeam, 2019).

Peak knee joint flexion was identified as the maximum knee flexion angle at the deepest point of the overhead squat motion. The corresponding knee frontal and transverse kinematics were determined and compared at this event, as peak knee flexion kinematics reflect the risk of knee injury (Hewett & Bates, 2017; McLean et al., 2005; Myer et al., 2015). The effect of marker sets and model constraint on the derived knee joint kinematic data at peak knee flexion were examined using two-way repeated measures ANOVAs. The assumption of sphericity was verified following the method of Girden (1992). Paired *t*-tests with Bonferroni correction with 95% CI were carried out to identify the mean differences between the four marker sets. One-way within-subject ANOVAs with Bonferroni correction examined any significant interaction. Partial η^2 was used to determine the effect size. The assumption of normality was checked by visual inspection of the histogram, q-q plot and the box plot of the data within the groups. Z-values of skewness and kurtosis and a Shapiro-Wilks test were also performed on the data. There were no violations of these assumptions. Statistical analyses were completed using the statistical software package SPSS (version 25, SPSS Inc., USA) with a significance level of $p < 0.05$.

Results:

The results for the mean of the time series for the right knee kinematics of all participants using the four marker sets and the 3 and 6DOF models are illustrated in Figures 3-5. The time series for the non-sagittal plane marker set and models demonstrate variation.

Figure 3 [insert here]

Figure 4 [insert here]

Figure 5 [insert here]

Sagittal plane

All RMSE values were below the suggested 5-degree threshold for error. The lowest RMSE between models was found between the Anterior Partial Cluster-3DOF (Ant-3DOF) and the Posterior Partial Cluster-3DOF models (Post-3DOF) (1.02 SD 1.08 degrees) with a cross correlation function of $r=0.99$ (SD 0.00). The largest RMSE was noted between the Posterior Partial Cluster knee-6DOF (Post-6DOF) (4.19 SD 1.41 degrees) and the Cluster-3DOF model (Clust-3DOF) with a cross correlation function of $r=0.99$ (SD 0.00). The calculated kinematic data for all the configurations in this plane correlated well (0.99) (See supplementary material).

At mean peak knee flexion, each of the marker set and DOF model combinations showed similar values (Figure 6). The 2-way ANOVA for repeated measurements in this plane revealed a significant main effect for marker set, ($F(1.77,15.92) = 6.00, p=0.014, \eta_p^2 = 0.40$). Pairwise comparisons revealed a significant difference only between the Anterior Partial Cluster and Cluster marker set of 2.43 degrees (95% CI [0.24, 4.62]). No significant main effects for DOF or the interaction between marker set and DOF were observed.

Figure 6 [insert here]

Frontal plane:

Lowest RMSE differences for the frontal plane were revealed between the Anterior Partial Cluster knee-6DOF (Ant-6DOF) and the Posterior Partial Cluster-6DOF models (Post-6DOF) (1.30 SD 0.93 degrees) with a cross-correlation function of $r=0.92$ (SD 0.09). Highest RMSE values were found between the Posterior-6DOF (Post-6DOF) and the Cluster-3DOF (6.39 SD 2.77 degrees) with a cross correlation function of $r=0.42$ (SD 0.36) (See supplementary material). The majority of configurations in this plane demonstrated lower agreement and differences > 5 degrees. Frontal plane kinematics at the moment of peak knee flexion are presented in Figure 7. A significant main effect was again noted for marker set, $F(2.06, 18.6) = 11.37, p=0.001, \eta_p^2 = 0.56$. Post hoc pairwise comparisons for the main effect of marker set showed that when comparing frontal plane angles at maximal knee flexion, significant mean differences were noted between the Anatomical and Anterior Partial Cluster marker sets (-2.22 degrees, 95%CI [-3.42, -1.01]), Anatomical and Posterior Partial Cluster (-3.89 degrees, 95% CI [-6.31, -1.47]) and Cluster and Posterior Partial Cluster (-3.83 degrees, 95% CI [-7.38, -0.28]) respectively. The Posterior partial cluster and both marker set models revealed mean rotations in opposite directions. No significant effects for DOF or interaction between marker set and DOF were observed.

Figure 7 [Insert here]

Transverse plane:

The RMSE was smallest between the Anterior Partial Cluster-6DOF (Ant-6DOF) and the Posterior partial Cluster-3DOF (Post-3DOF) (1.33 SD 0.56 degrees), with a cross correlation function of $r=0.92$ (SD 0.08). The largest difference was found between the Posterior partial Cluster-6DOF (Post-6DOF) and the Cluster 4-3DOF models (Clust-3DOF) (7.97 RMSE SD 2.66 degrees), with a cross correlation function of $r=0.65$ (SD 0.31). Many of the models in this plane revealed lower agreement and differences greater than 5 degrees (See supplementary material).

A significant interaction was observed between both marker set and DOF in this plane ($F(1.33,12.00) = 13.05$, $p=0.002$, $\eta_p^2=0.59$) (see Figure 8). Further examination using paired t-tests and one-way repeated measures ANOVAs revealed significantly higher mean differences for the 6DOF versus 3DOF models for the Anatomical (3.59, 95%CI [0.49, 6.69] degrees) and Cluster marker sets (3.03, 95%CI [1.06, 4.99] degrees) respectively. While the Posterior Partial Cluster (6DOF) revealed significantly lower values compared with the 3DOF model (mean difference -3.67, 95%CI [-5.83, -1.51] degrees). A one-way repeated measures ANOVA comparing all marker set (6DOF) models was also significant, $F(1.65,14.87) = 93.46$, $p<0.001$, $\eta_p^2=0.91$. Pairwise comparisons of the 6DOF models highlighted significant differences between all marker sets except between the Anterior Partial Cluster and Posterior Partial Cluster marker sets. These 6DOF significant differences ranged from the lowest mean difference between the Anatomical and Anterior Partial Cluster of 2.01 degrees, 95% CI [0.78, 3.24], to the highest mean difference of 7.31 degrees, 95% CI [5.08, 9.54] between the Anterior Cluster and Cluster 6DOF pairs. For the 3DOF models there was also a significant main effect for marker set, $F(1.40,12.61) = 5.75$, $p=0.024$, $\eta_p^2=0.39$. However, a significant difference was only observed between the Anterior Partial Cluster (Ant3DOF) and Cluster (Clust3DOF) (3.85 degrees, 95%CI [1.79, 5.91] models. A large SD was evident for all marker sets in this plane (Figure 8).

Figure 8[insert here]

Discussion and Implications :

This study explored the influence of four different marker sets using both 3DOF and 6DOF models on the derived knee kinematic data during the bilateral overhead squat in elite youth footballers. The sagittal plane results at peak knee flexion showed similar mean values below the suggested kinematic fidelity threshold of 5-degrees for motion capture error (McGinley et al., 2009; Slater et al., 2018) with low RMSE values and excellent correlation. However, significant differences were revealed between the Anterior Partial Cluster and Cluster marker sets (2.43 degrees).

In this study, the difficulty in evaluating the quality of movement during the overhead squat in the frontal and transverse plane due to marker set and model configuration is highlighted by the differences at peak knee flexion being greater than the suggested 5-degree threshold of agreement, with higher RMSE and lower cross correlation function values. The frontal plane kinematics demonstrated significant differences between the Anatomical and both the Anterior Partial Cluster and posterior partial cluster respectively, and between the Cluster and Posterior partial cluster marker sets. The findings in the transverse plane, revealed many large differences, a large SD variation and a significant interaction for marker set and DOF. Our results reflect other studies where the combination of smaller angles and difficulty tracking both these planar motions was reported (Andersen et al., 2010; Duffell et al., 2014; Richard et al., 2017), in particular during the quasi-squat (Clément, de Guise, Fuentes, & Hagemeister, 2018; Clément, Dumas, Hagemeister, & de Guise, 2015). Moreover, the frontal and transverse plane results at peak knee flexion revealed physiologically implausible kinematic data specifically for the Anatomical (6DOF), Cluster, and Posterior partial-cluster marker sets, when considered using the benchmark of gold standard validated motion (Bennett, Fleenor, & Weinhandl, 2018; Benoit et al., 2006; Donohue et al., 2015; Philp et al., 2019; Potvin et al., 2017; Richard et al., 2017; Sangeux, Barré, & Aminian, 2017; Sauret, Pillet, Skalli, & Sangeux, 2016; Smale et al., 2017). Based on these results, these marker sets do not appear to provide valid calculated knee kinematic data for tracking a larger range of motion task in an athletic population.

The cluster marker set findings conflict with the existing recommendations, which have suggested that the use of clusters helps to reduce the kinematic error (Buczek et al., 2010; Collins et al., 2009). The cluster marker sets using both 3DOF and 6DOF performed poorly when tracking the frontal and transverse plane motion, with high RMSE values (frontal plane; 4-5 degrees, transverse plane; RMSE > 5 degrees) and poorer cross correlation values, in agreement with (Mentiplay & Clark, 2018). Further, recent results mapping soft-tissue artefact distribution suggest that marker clusters do not compensate for the kinematic error, particularly in the thigh (Barré, Jolles, Theumann, & Aminian, 2015). However, the Anatomical marker set which excluded the thigh cluster markers did not compare well with other models in this study, in contrast to previous findings (Mantovani & Lamontagne, 2017; Schulz & Kimmel, 2010; Slater et al., 2018). Using a four marker cluster with no additional tracking markers, or markers which are defined solely by anatomical structures did not appear to be an optimal solution for assessing the overhead squat movement in an athletic population.

Reaching consensus on the optimal modelling solution during the overhead squat, particularly in the transverse plane, is difficult. Constraining the knee joint motion to 3DOF revealed significant differences between only one pair of marker sets and suggests that this may be the solution to improve data fidelity during the overhead squat supported by some previous findings (Andersen et al., 2010; Duprey et al., 2010). The lower mean differences between marker sets in 6DOF found in this study suggested that the 6DOF models may be superior. However, the 6DOF marker set comparison revealed all three marker sets were significantly different in contrast to some previous findings (Buczek et al.,

2010; Fiorentino et al., 2017; Mentiplay & Clark, 2018; Potvin et al., 2017). The transverse plane DOF, pairwise comparisons between 3DOF and 6DOF models, revealed significant differences for all marker sets except the anterior partial cluster models, which is of interest given the larger thigh muscle mass in trained athletic populations (Milsom et al., 2015; Peek, Gatherer, Bennett, Fransen, & Watsford, 2018). These results highlight the importance of DOF constraints, particularly in the transverse plane for future research and corroborate the findings of (Schellenberg, Taylor, Jonkers, & Lorenzetti, 2017). The findings suggest that future investigation of marker location and biomechanical modelling during other commonly assessed athletic movement tasks, including more dynamic movement tests, is required in order to improve the fidelity and usefulness of derived data using marker-based 3D motion capture. Further, the nature of participants could be a determining factor in the selection of marker locations and joint constraints.

There are limitations to this study, including the small sample size and the reliance upon consistent marker placement for accurate joint definitions between participants. Marker set crosstalk was not controlled for in this study (Smale et al., 2017). The absence of direct skeletal measurement using the gold standard, despite these methods underestimating abnormal kinematics, is an additional limitation (Akbarshahi et al., 2010; Li, Zheng, Tashman, & Zhang, 2012). The overhead squat in this study was performed at a relatively slow velocity, which may not be representative of more dynamic tasks and which may result in different outcomes.

Conclusion

Marker location and model configuration are important considerations when assessing athletic movement tasks. The significant differences between marker sets and model combinations during the overhead squat at peak knee flexion, particularly in the frontal and transverse planes highlight these inconsistencies. Therefore, caution is needed when comparing studies using different marker sets, models, motion tasks or populations. While it was out with the scope of this study to determine an optimal configuration for this population, primarily due to the inability to compare with reliable alternative tools, the Anterior Partial-Cluster using either the 3DOF or 6DOF models, appeared to be the most robust method for analysing knee rotational kinematics during the overhead squat in an athletic population. The benefit of not constraining DOF may also be useful in practice and research where joint translations are of interest. Further, these results suggest further research is necessary concerning marker set and model when assessing more dynamic athletic movement tasks, particularly for research into the mitigation of lower limb injury risk.

Word count (text) 4, 230

Conflict of Interest Statement

The authors of this manuscript did not have any conflicts of interest related to this study.

Acknowledgements

The authors of this manuscript would like to thank Arsenal Academy Sports Science and Sports Medicine Department and Dr. Alan McCall for assistance with this paper.

Funding

This work was supported by Science Foundation Ireland under grant number SFI/12/RC/2289 (Insight).

References

- Akbarshahi, M., Schache, A. G., Fernandez, J. W., Baker, R., Banks, S., & Pandy, M. G. (2010). Non-invasive assessment of soft-tissue artifact and its effect on knee joint kinematics during functional activity. *Journal of Biomechanics*, 43(7), 1292-1301.
- Andersen, M. S., Benoit, D. L., Damsgaard, M., Ramsey, D. K., & Rasmussen, J. (2010). Do kinematic models reduce the effects of soft tissue artefacts in skin marker-based motion analysis? An in vivo study of knee kinematics. *Journal of Biomechanics*, 43(2), 268-273.
- Ardern, C. L., Ekås, G., Grindem, H., Moksnes, H., Anderson, A., Chotel, F., Cohen, M., Forssblad, M., Ganley, T.J., Feller, J.A., Karlsson, J., Kocher, M.S., LaPrade, R. F., McNamee, M., Mandelbaum, B., Micheli, L., Mohtadi, N., Reider, B., Roe, J., Seil, R., ... Engebretsen, L. (2018). 2018 International Olympic Committee consensus statement on prevention, diagnosis and management of paediatric anterior cruciate ligament (ACL) injuries. *Knee surgery, sports traumatology, arthroscopy : official journal of the ESSKA*, 26(4), 989–1010. <https://doi.org/10.1007/s00167-018-4865-y>
- Bagwell, J. J., Snibbe, J., Gerhardt, M., & Powers, C. M. (2016). Hip kinematics and kinetics in persons with and without cam femoroacetabular impingement during a deep squat task. *Clinical Biomechanics* (Bristol, Avon), 31, 87-92. doi:10.1016/j.clinbiomech.2015.09.016
- Baker, R., Leboeuf, F., Reay, J., & Sangeux, M. (2017). The Conventional Gait Model - Success and Limitations. In B. Müller, S. I. Wolf, G.-P. Brueggemann, Z. Deng, A. McIntosh, F. Miller, & W. S. Selbie (Eds.), *Handbook of Human Motion* (pp. 1-19). Cham: Springer International Publishing.
- Barré, A., Jolles, B. M., Theumann, N., & Aminian, K. (2015). Soft tissue artifact distribution on lower limbs during treadmill gait: Influence of skin markers' location on cluster design. *Journal of Biomechanics*, 48(10), 1965-1971. doi:10.1016/j.jbiomech.2015.04.007
- Baxter, J. R., Sturnick, D. R., Demetracopoulos, C. A., Ellis, S. J., & Deland, J. T. (2016). Cadaveric gait simulation reproduces foot and ankle kinematics from population-specific inputs. *Journal of Orthopaedic Research*, 34(9), 1663-1668.
- Bennett, H. J., Fleenor, K., & Weinhandl, J. T. (2018). A normative database of hip and knee joint biomechanics during dynamic tasks using anatomical regression prediction methods. *Journal of Biomechanics*, 81, 122-131. doi:https://doi.org/10.1016/j.jbiomech.2018.10.003
- Benoit, D. L., Ramsey, D. K., Lamontagne, M., Xu, L., Wretenberg, P., & Renström, P. (2006). Effect of skin movement artifact on knee kinematics during gait and cutting motions measured in vivo. *Gait & posture*, 24(2), 152-164. doi:https://doi.org/10.1016/j.gaitpost.2005.04.012
- Bergeron, M.F., Mountjoy, M., Armstrong, N., Chia, M., Côté, J., Emery, C.A., Faigenbaum, A., Hall, G., Kriemler, S., Léglise, M. and Malina, R.M., 2015. International Olympic Committee consensus statement on youth athletic development. *British Journal of Sports Medicine*, 49(13), 843-851.
- Bishop, C., Edwards, M., & Turner, A. N. (2016). Screening movement dysfunctions using the overhead squat. *Professional Strength & Conditioning*, 42, 22-30.
- Bishop, C., Villiere, A., & Turner, A. (2016). Addressing movement patterns by using the overhead squat. *Professional Strength & Conditioning*, 40, 7-12.
- Buczek, F. L., Rainbow, M. J., Cooney, K. M., Walker, M. R., & Sanders, J. O. (2010). Implications of using hierarchical and six degree-of-freedom models for normal gait analyses. *Gait & posture*, 31(1), 57-63.

- Clément, J., de Guise, J. A., Fuentes, A., & Hagemester, N. (2018). Comparison of soft tissue artifact and its effects on knee kinematics between non-obese and obese subjects performing a squatting activity recorded using an exoskeleton. *Gait & posture*, 61, 197-203. doi:<https://doi.org/10.1016/j.gaitpost.2018.01.009>
- Clément, J., Dumas, R., Hagemester, N., & de Guise, J. A. (2015). Soft tissue artifact compensation in knee kinematics by multi-body optimization: Performance of subject-specific knee joint models. *Journal of Biomechanics*, 48(14), 3796-3802. doi:<https://doi.org/10.1016/j.jbiomech.2015.09.040>
- Cockcroft, J., Louw, Q., & Baker, R. (2016). Proximal placement of lateral thigh skin markers reduces soft tissue artefact during normal gait using the Conventional Gait Model. *Computer Methods Biomechanical Biomedical Engineering*, 19(14), 1497-1504. doi:10.1080/10255842.2016.1157865
- Collins, T. D., Ghousayni, S. N., Ewins, D. J., & Kent, J. A. (2009). A six degrees-of-freedom marker set for gait analysis: repeatability and comparison with a modified Helen Hayes set. *Gait & posture*, 30(2), 173-180.
- Cook, G., Burton, L., & Hoogenboom, B. (2006). Pre-participation screening: the use of fundamental movements as an assessment of function-part 1. *North American journal of sports physical therapy: NAJSPT*, 1(2), 62-72.
- Cortes, N., Greska, E., Ambegaonkar, J. P., Kollock, R. O., Caswell, S. V., & Onate, J. A. (2014). Knee kinematics is altered post-fatigue while performing a crossover task. *Knee Surgery, Sports Traumatology, Arthroscopy*, 22(9), 2202-2208.
- Donohue, M. R., Ellis, S. M., Heinbaugh, E. M., Stephenson, M. L., Zhu, Q., & Dai, B. (2015). Differences and correlations in knee and hip mechanics during single-leg landing, single-leg squat, double-leg landing, and double-leg squat tasks. *Research in sports medicine*, 23(4), 394-411.
- Duffell, L. D., Hope, N., & McGregor, A. H. (2014). Comparison of kinematic and kinetic parameters calculated using a cluster-based model and Vicon's plug-in gait. Proceedings of the Institution of Mechanical Engineers. Part H, Journal of engineering in medicine, 228(2), 206–210. doi:10.1177/0954411913518747
- Duprey, S., Cheze, L., & Dumas, R. (2010). Influence of joint constraints on lower limb kinematics estimation from skin markers using global optimization. *Journal of Biomechanics*, 43, 2858-2862.
- Fiorentino, N. M., Atkins, P. R., Kutschke, M. J., Goebel, J. M., Foreman, K. B., & Anderson, A. E. (2017). Soft tissue artifact causes significant errors in the calculation of joint angles and range of motion at the hip. *Gait & posture*, 55, 184-190. doi:10.1016/j.gaitpost.2017.03.033
- Gasparutto, X., Sancisi, N., Jacquelin, E., Parenti-Castelli, V., & Dumas, R. (2015). Validation of a multi-body optimization with knee kinematic models including ligament constraints. *Journal of Biomechanics*, 48(6), 1141-1146.
- Hewett, T. E., & Bates, N. A. (2017). Preventive biomechanics: a paradigm shift with a translational approach to injury prevention. *The American journal of sports medicine*, 45(11), 2654-2664.
- Khamis, H. J., & Roche, A. F. (1994). Predicting adult stature without using skeletal age: the Khamis-Roche method. *Pediatrics*, 94(4), 504-507.
- Lees, A., Asai, T., Andersen, H., Nunome, H., & Stetzing, T. (2010). The biomechanics of kicking in soccer: A review. *Journal of Sports Sciences*, 28(8), 805-817.
- Leporace, G., Praxedes, J., Pereira, G.R., Pinto, S.M., Chagas, D., Metsavaht, L., Chame, F. and Batista, L.A., 2013. Influence of a preventive training program on lower limb kinematics and vertical jump height of male volleyball athletes. *Physical Therapy in Sport*, 14(1), 35-43.
- Li, K., Zheng, L., Tashman, S., & Zhang, X. (2012). The inaccuracy of surface-measured model-derived tibiofemoral kinematics. *Journal of Biomechanics*, 45(15), 2719-2723. doi:<https://doi.org/10.1016/j.jbiomech.2012.08.007>

- Lu, T. W., & O' Connor, J. J. (1999). Bone position estimation from skin marker co-ordinates using global optimisation with joint constraints. *Journal of Biomechanics*, 32(2), 129-134.
- Malina, R. M., Rogol, A. D., & Cumming, S. P. (2015). Biological maturation of youth athletes: assessment and implications. *British Journal of Sports Medicine*, 49(13), 852-859.
- Mantovani, G., & Lamontagne, M. (2017). How different marker sets affect joint angles in inverse kinematics framework. *Journal of biomechanical engineering*, 139(4).
- Marques, V. B., Medeiros, T. M., de Souza Stigger, F., Nakamura, F. Y., & Baroni, B. M. (2017). The Functional Movement Screen (FMS™) in elite young soccer players between 14 and 20 years : Composite scores, individual-test scores and asymmetries. *International journal of sports physical therapy*, 12(6), 977–985. doi:10.16603/ijsp20170977
- McCall, A., Carling, C., Davison, M., Nedelec, M., Le Gall, F., Berthoin, S., & Dupont, G. (2015). Injury risk factors, screening tests and preventative strategies: a systematic review of the evidence that underpins the perceptions and practices of 44 football (soccer) teams from various premier leagues. *British Journal of Sports Medicine*, 49(9), 583-589.
- McCall, A., Lewin, C., O'Driscoll, G., Witvrouw, E., & Ardern, C. (2017). Return to play: the challenge of balancing research and practice. *British Journal of Sports Medicine*, 51(9), 702-703.
- McFadden, C., Daniels, K., & Strike, S. (2020). The sensitivity of joint kinematics and kinetics to marker placement during a change of direction task. *Journal of Biomechanics*, 101, 109635. doi:https://doi.org/10.1016/j.jbiomech.2020.109635
- McGinley, J. L., Baker, R., Wolfe, R., & Morris, M. E. (2009). The reliability of three-dimensional kinematic gait measurements: a systematic review. *Gait & posture*, 29(3), 360-369. doi:10.1016/j.gaitpost.2008.09.003
- McLean, S. G., Walker, K., Ford, K., Myer, G., Hewett, T., & van den Bogert, A. J. (2005). Evaluation of a two dimensional analysis method as a screening and evaluation tool for anterior cruciate ligament injury. *British Journal of Sports Medicine*, 39(6), 355-362.
- Mentiplay, B. F., & Clark, R. A. (2018). Modified conventional gait model versus cluster tracking: test-retest reliability, agreement and impact of inverse kinematics with joint constraints on kinematic and kinetic data. *Gait & posture*, 64, 75-83.
- Milsom, J., Naughton, R., O'Boyle, A., Iqbal, Z., Morgans, R., Drust, B., & Morton, J. P. (2015). Body composition assessment of English Premier League soccer players: a comparative DXA analysis of first team, U21 and U18 squads. *Journal of Sports Sciences*, 33(17), 1799-1806. doi:10.1080/02640414.2015.1012101
- Myer, G. D., Ford, K. R., Di Stasi, S. L., Foss, K. D. B., Micheli, L. J., & Hewett, T. E. (2015). High knee abduction moments are common risk factors for patellofemoral pain (PFP) and anterior cruciate ligament (ACL) injury in girls: is PFP itself a predictor for subsequent ACL injury?. *British Journal of Sports Medicine*, 49(2), 118-122.
- Ojeda, J., Martínez-Reina, J., & Mayo, J. (2014). A method to evaluate human skeletal models using marker residuals and global optimization. *Mechanism and Machine Theory*, 73, 259-272.
- Onate, J. A., Dewey, T., Kollock, R. O., Thomas, K. S., Van Lunen, B. L., DeMaio, M., & Ringleb, S. I. (2012). Real-time intersession and interrater reliability of the functional movement screen. *The Journal of Strength & Conditioning Research*, 26(2), 408-415.
- Peek, K., Gatherer, D., Bennett, K. J. M., Franssen, J., & Watsford, M. (2018). Muscle strength characteristics of the hamstrings and quadriceps in players from a high-level youth football (soccer) Academy. *Research in sports medicine*, 26(3), 276-288. doi:10.1080/15438627.2018.1447475
- Philp, F., Leboeuf, F., Pandyan, A., & Stewart, C. (2019). "Dynamic knee valgus" - Are we measuring what we think we're measuring? An evaluation of static and functional knee calibration methods for application in gait and clinical screening tests of the overhead squat and hurdle step. *Gait & posture*, 70, 298-304. doi:10.1016/j.gaitpost.2019.03.006

- Potvin, B. M., Shourijeh, M. S., Smale, K. B., & Benoit, D. L. (2017). A practical solution to reduce soft tissue artifact error at the knee using adaptive kinematic constraints. *Journal of Biomechanics*, 62, 124-131.
- R CoreTeam. (2019). R: A language and environment for statistical computing. Vienna, Austria: R Foundation for Statistical Computing <https://www.R-project.org/>.
- Richard, V., Cappozzo, A., & Dumas, R. (2017). Comparative assessment of knee joint models used in multi-body kinematics optimisation for soft tissue artefact compensation. *Journal of Biomechanics*, 62, 95-101.
- Robinson, M. A., Donnelly, C. J., Tsao, J., & Vanrenterghem, J. (2013). Impact of knee modeling approach on indicators and classification of ACL injury risk. *Medicine and science in sports and exercise*, 46, 1269-1276.
- Ryan, D., Lewin, C., Forsythe, S., & McCall, A. (2018). Developing World-Class Soccer Players: An Example of the Academy Physical Development Program From an English Premier League Team. *Strength & Conditioning Journal*, 40(3), 2-11. doi:10.1519/ssc.0000000000000340
- Sangeux, M., Barré, A., & Aminian, K. (2017). Evaluation of knee functional calibration with and without the effect of soft tissue artefact. *Journal of Biomechanics*, 62, 53-59. doi:<https://doi.org/10.1016/j.jbiomech.2016.10.049>
- Sauret, C., Pillet, H., Skalli, W., & Sangeux, M. (2016). On the use of knee functional calibration to determine the medio-lateral axis of the femur in gait analysis: Comparison with EOS biplanar radiographs as reference. *Gait & Posture*, 50, 180-184. doi:10.1016/j.gaitpost.2016.09.008
- Schache, A. G., Baker, R., & Lamoreux, L. W. (2008). Influence of thigh cluster configuration on the estimation of hip axial rotation. *Gait & posture*, 27(1), 60-69.
- Schellenberg, F., Taylor, W. R., Jonkers, I., & Lorenzetti, S. (2017). Robustness of kinematic weighting and scaling concepts for musculoskeletal simulation. *Computer Methods in Biomechanics and Biomedical Engineering*, 20(7), 720-729.
- Schmitz, A., Buczek, F. L., Bruening, D., Rainbow, M. J., Cooney, K., & Thelen, D. (2016). Comparison of hierarchical and six degrees-of-freedom marker sets in analyzing gait kinematics. *Computer Methods in Biomechanics and Biomedical Engineering*, 19(2), 199-207.
- Schoenfeld, B. J. (2010). Squatting kinematics and kinetics and their application to exercise performance. *The Journal of Strength & Conditioning Research*, 24(12), 3497-3506.
- Schulz, B. W., & Kimmel, W. L. (2010). Can hip and knee kinematics be improved by eliminating thigh markers? *Clinical Biomechanics*, 25(7), 687-692.
- Scibek, E. P., Moran, M. F., & Edmond, S. L. (2020). Accuracy of Functional Movement Screen Deep Squat Scoring and the Influence of Optimized Scoring Criteria: A 3-Dimensional Kinematic Approach. *Journal of sport rehabilitation*, 1(aop), 1-7.
- Slater, A. A., Hullfish, T. J., & Baxter, J. R. (2018). The Impact Of Thigh And Shank Marker Quantity On Lower Extremity Kinematics Using A Constrained Model. *BMC Musculoskeletal Disorders*, 19(399), 1-10.
- Smale, K. B., Potvin, B. M., Shourijeh, M. S., & Benoit, D. L. (2017). Knee joint kinematics and kinetics during the hop and cut after soft tissue artifact suppression: Time to reconsider ACL injury mechanisms? *Journal of Biomechanics*, 62, 132-139. doi:10.1016/j.jbiomech.2017.06.049
- Wen, Y., Huang, H., Yu, Y., Zhang, S., Yang, J., Ao, Y., & Xia, S. (2018). Effect of tibia marker placement on knee joint kinematic analysis. *Gait & posture*, 60, 99-103. <https://doi.org/10.1016/j.gaitpost.2017.11.020>
- Whittaker, J.L., Booyesen, N., De La Motte, S., Dennett, L., Lewis, C.L., Wilson, D., McKay, C., Warner, M., Padua, D., Emery, C.A. and Stokes, M., 2017. Predicting sport and occupational lower extremity injury risk through movement quality screening: a systematic review. *British Journal of Sports Medicine*, 51(7), 580-585.

Žuk, M., & Pezowicz, C. (2015). Kinematic Analysis of a Six-Degrees-of-Freedom Model Based on ISB Recommendation: A Repeatability Analysis and Comparison with Conventional Gait Model. *Applied Bionics and Biomechanics*, 2015, 503713. doi:10.1155/2015/503713

Figure 1a) : Full lower limb marker sets detailing the cluster with medial and lateral knee joint markers. The SCS for the knee joint axes was aligned with (X) positive axis in mediolateral direction, positive (Y) axis anterior/posterior and positive (Z) axis vertical directions respectively.

Figure 1b) : Full thigh four marker cluster detailing the Anterior partial cluster (grey), Posterior partial cluster (white) markers that were used with medial and lateral knee joint markers

Figure 2 : Bilateral overhead squat movement test to compare marker set and models.

Figure 3 : Group mean (n=10) of the full time-series for the overhead squat in the sagittal plane using the four marker sets and both model configurations (3DOF, 6DOF). The right knee flexion angles are negative.

Figure 4 : Group mean of the full time series for the overhead squat in the frontal plane for the four marker sets and both DOF model configurations (3DOF, 6DOF). Abduction (negative) and adduction (positive) angles.

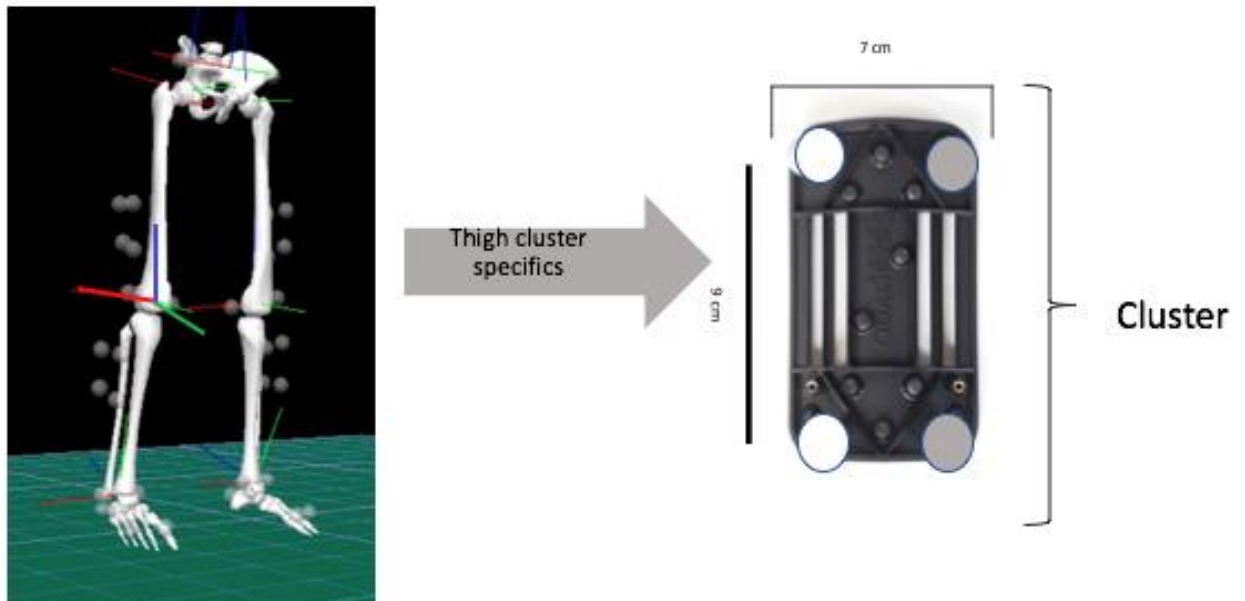
Figure 5: Group mean of the full time series for the overhead squat in the transverse plane for all four marker sets and both model configurations (3DOF, 6DOF). Internal rotation (positive) and external rotation (negative) angles.

Figure 6: Mean Peak flexion angles in the sagittal plane for the overhead squat using all four marker sets and both model configurations (6DOF, 3DOF). Flexion (negative) and extension (positive) angles. Examination of the significant main effect for marker set in the pairwise comparisons showed only a significant difference between the Anterior Partial Cluster (AntClusterKnee) and Cluster marker sets, averaged over DOF models.

Figure 7: Mean frontal plane angles at the peak knee flexion event during the overhead squat, using four marker sets and both models (6DOF and 3DOF). Abduction (negative) and adduction (positive) angles. Examination of the significant main effect for marker set, revealed significant differences between the anatomical, anterior partial cluster and the posterior partial cluster respectively and cluster and posterior cluster marker sets. No significant effect was noted for DOF. The posterior partial cluster marker sets by DOF model revealed rotations in opposing directions.

Figure 8: Mean transverse plane angles at the peak knee flexion event during the overhead squat for all four marker set and both models (6DOF and 3DOF). Internal rotation (positive)

and external rotation (negative) angles. The P-values are indicated for the significant comparisons based on the significant interaction between marker set and DOF model. Significant differences between the 6DOF and 3DOF models were noted between all marker sets except the Anterior Cluster (AntClusterKnee). For all 3DOF models (lighter coloured bar chart) only significant differences were noted between the AntClusterKnee and Cluster marker sets. Large SD were revealed for all models in this plane



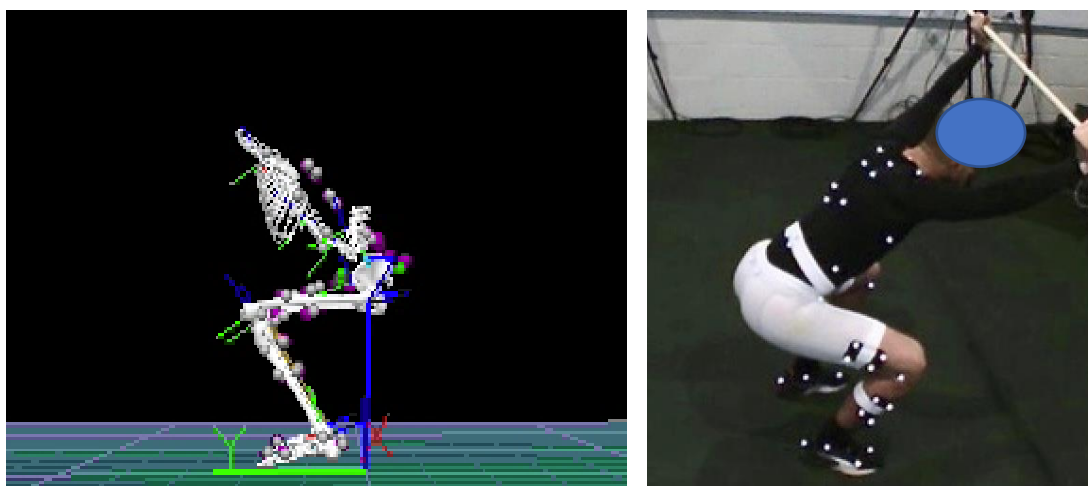
640

641 1a) Full lower limb marker sets detailing the cluster with medial and lateral knee joint markers.
 642 The SCS for the knee joint axes was aligned with (X) positive axis in mediolateral direction,
 643 positive (Y) axis anterior/posterior and positive (Z) axis vertical directions respectively.

644 1b) Full thigh four marker cluster also detailing the Anterior partial cluster (grey), Posterior
 645 partial cluster (white) makers that were used with medial and lateral knee joint markers.

646

647



648

649

650 Figure 2 : Bilateral overhead squat movement test to compare marker set and models.

651

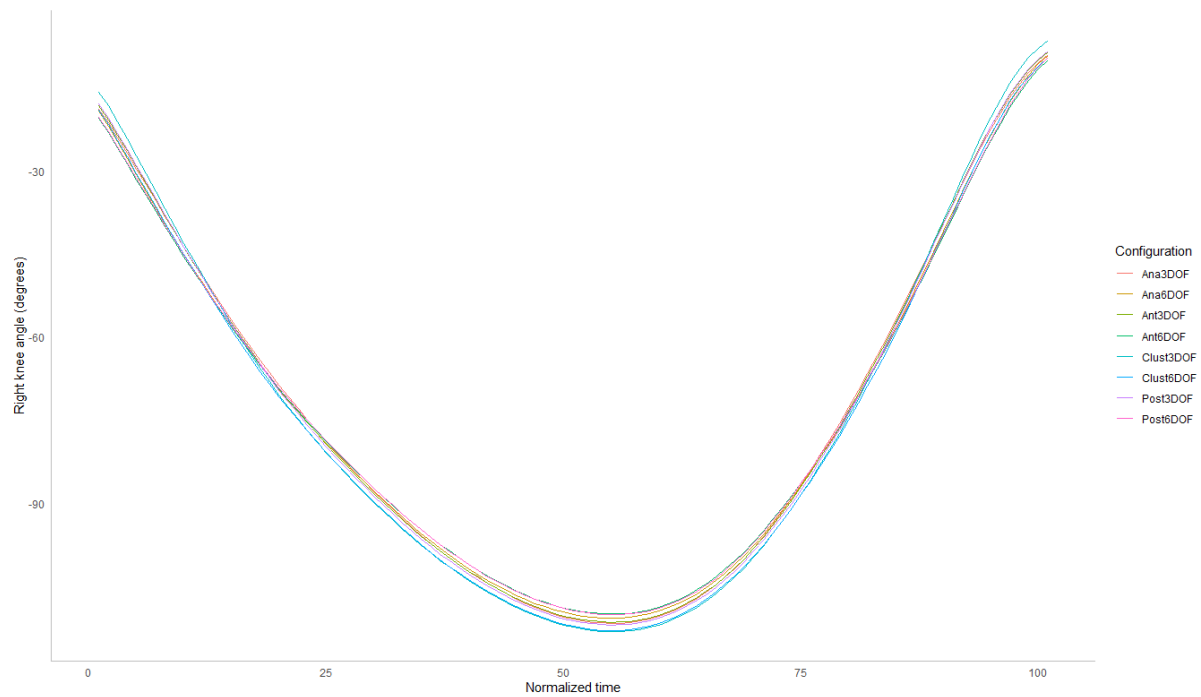


Figure 3: Group mean (n=10) of the full time-series for the overhead squat in the sagittal plane using the four marker sets and two model (3DOF, 6DOF) configurations. The right knee flexion angle is negative.

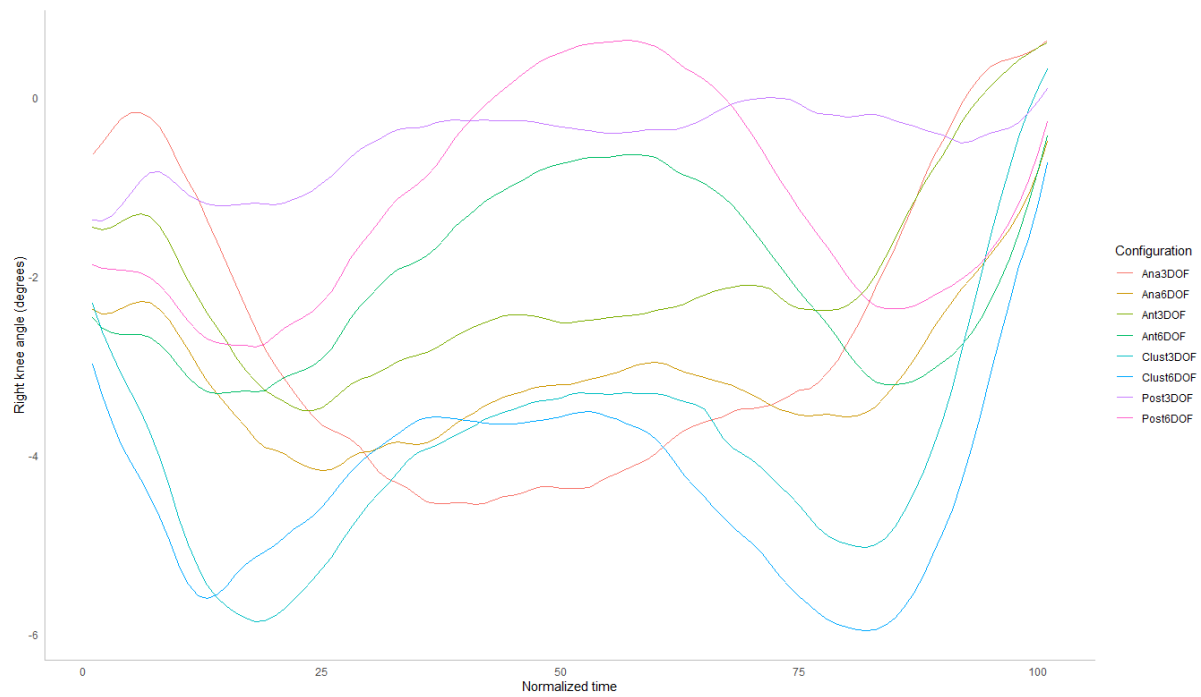


Figure 4: The group mean full time series of the overhead squat in the frontal plane for the four marker sets and both DOF model (3DOF, 6DOF) configurations. Abduction (negative) and adduction (positive) angles.

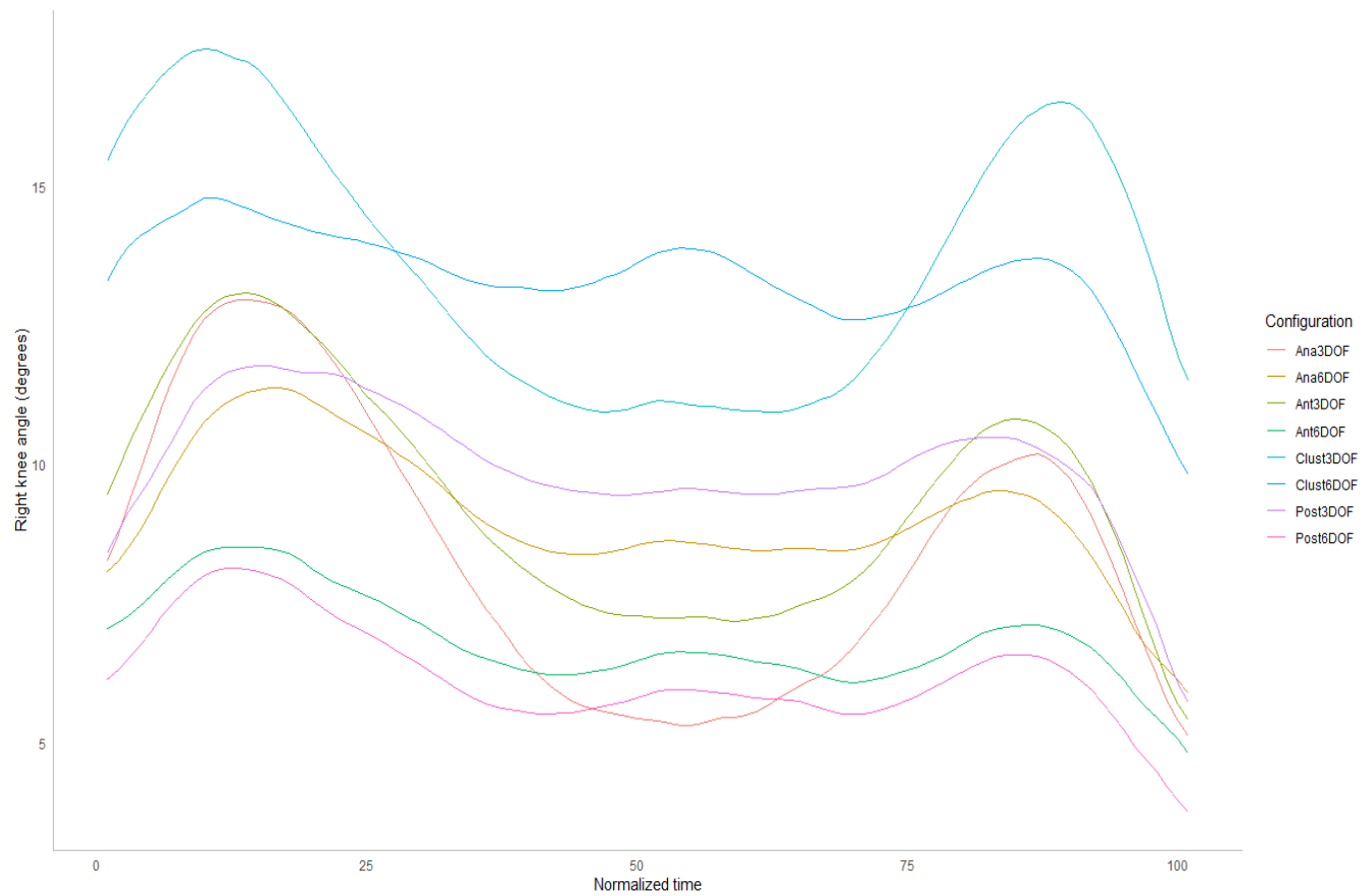
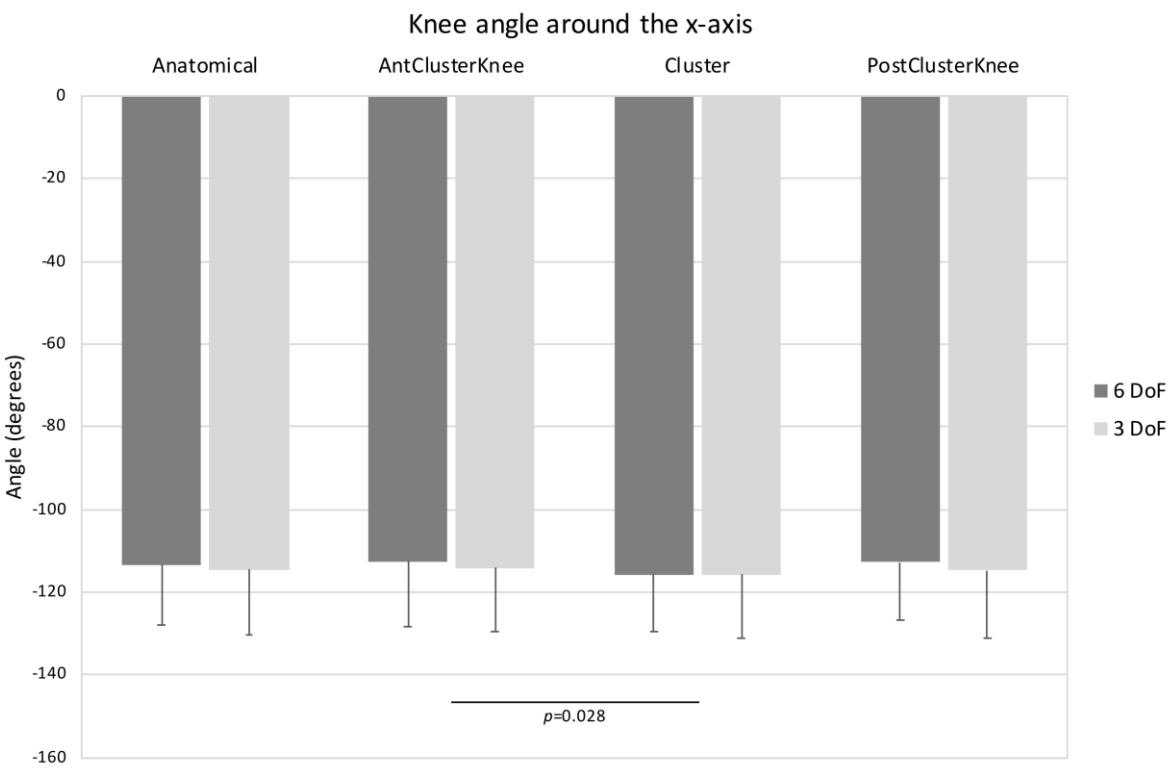


Figure 5: Group mean full time series for the overhead squat in the transverse plane for all four marker sets and both model (3DOF, 6DOF) configurations. Internal rotation (positive) and external rotation (negative) angles.



670

671 **Figure 6:** Mean Peak flexion angles in the sagittal plane for the overhead squat using all four
672 marker sets and both model configurations (6DOF, 3DOF). Flexion negative angles, and
673 extension positive angles. Examination of the significant main effect for marker set in the
674 pairwise comparisons, showed only a significant difference between the Anterior Partial
675 Cluster (AntClusterKnee) and Cluster marker sets, averaged over DOF models.

676

677

678

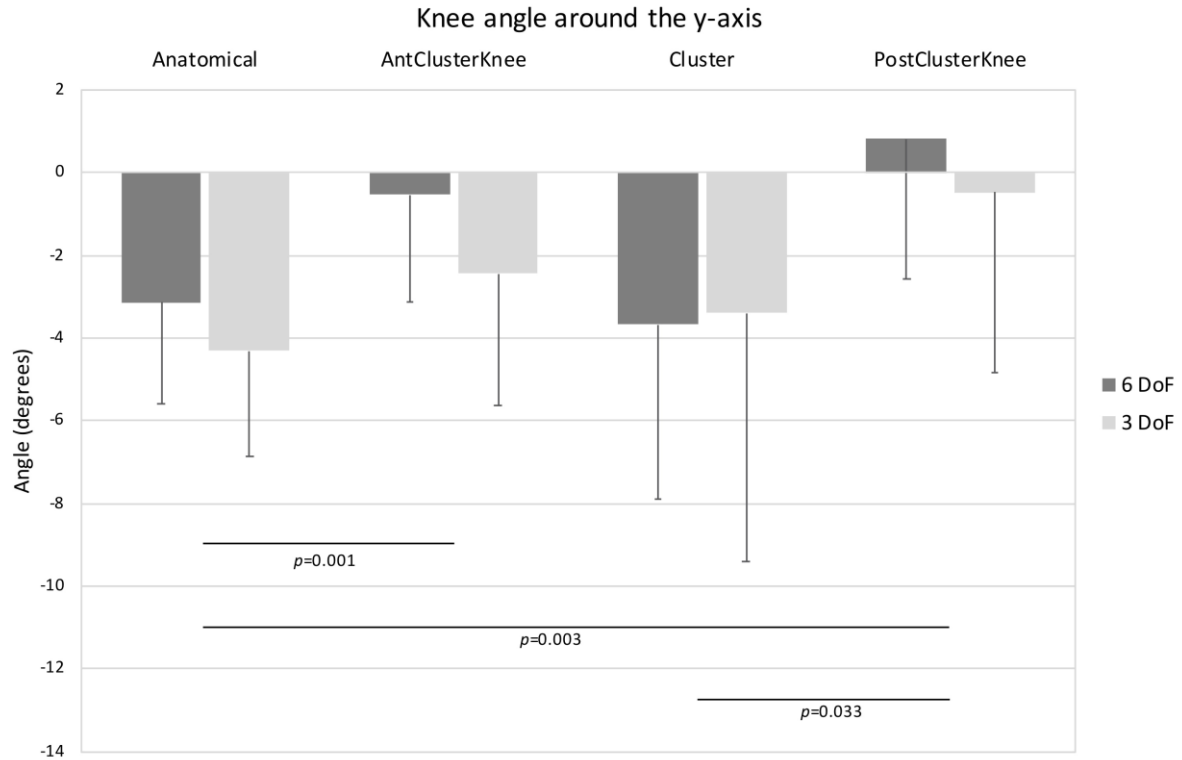


Figure 7: Mean frontal plane angles at the peak knee flexion event during the overhead squat, using four marker sets and both models (6DOF and 3DOF). Abduction angles are negative and adduction angles are positive. Examination of the significant main effect for marker set, revealed significant differences between the anatomical, anterior partial cluster and the posterior partial cluster respectively and cluster and posterior cluster marker sets. No significant effect was noted for DOF. The posterior partial cluster marker sets by DOF model revealed rotations in opposing directions.

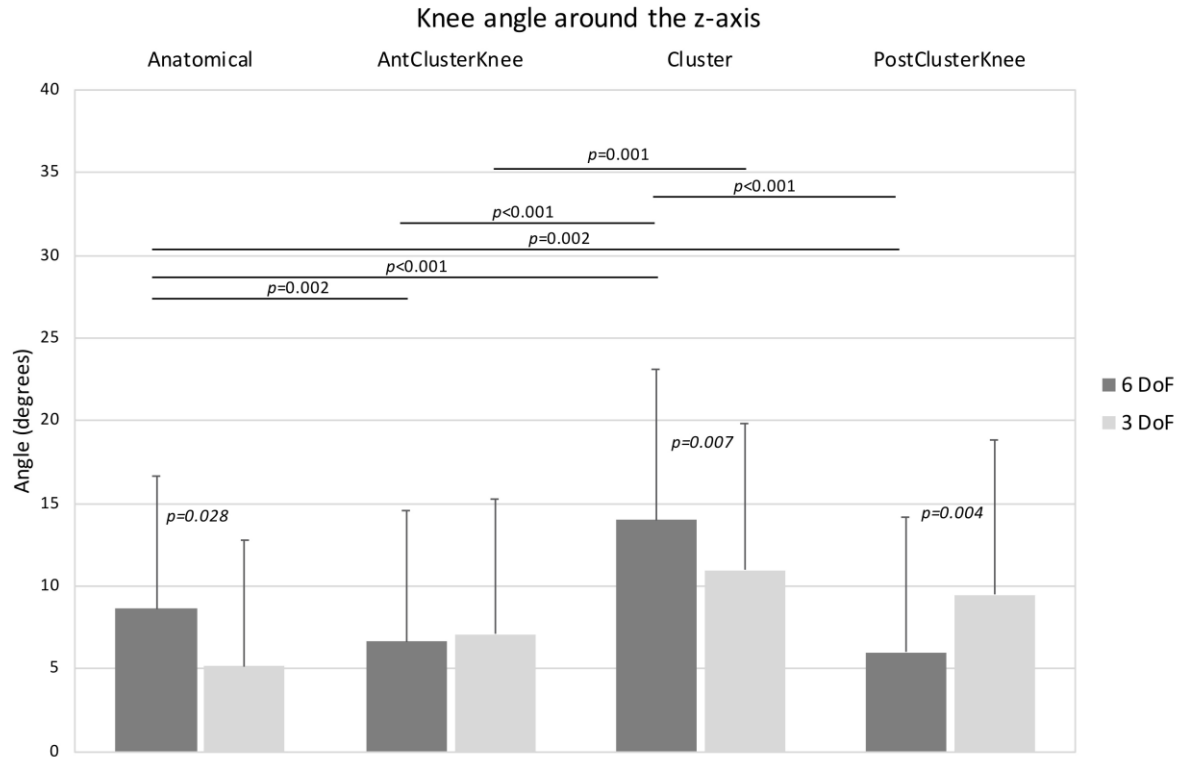


Figure 8: Mean transverse plane angles at the peak knee flexion event during the overhead squat for all four marker set and both models (6DOF and 3DOF). Internal rotation positive angles and external rotation negative angles. The P-values are indicated for the significant comparisons based on the significant interaction between marker set and DOF model. Significant differences between the 6DOF and 3DOF models were noted between all marker sets except the Anterior Cluster(AntClusterKnee). For all 3DOF models (lighter coloured bar chart) only significant differences were noted between the AntClusterKnee and Cluster marker sets. Large SD were revealed for all models in this plane.

709 **Appendix 1:** Sagittal plane results for RMSE between all eight marker sets in the upper section of table and cross-correlation values in the lower section of
710 table. For each trial, RMSE and cross-correlation values were calculated for each combination comparison between two of the eight marker sets. Values
711 were first averaged over the three repeated trials within the participants. Finally, the group mean (N=10) values and standard deviations were calculated
712 over these individual means, which are presented in this table.

713

714

	Right_knee_angle_x_Anatomical	Right_knee_angle_x_Anatomical SD	Right_knee_angle_x_AntClusterKnee	Right_knee_angle_x_AntClusterKnee SD	Right_knee_angle_x_Cluster4	Right_knee_angle_x_Cluster4 SD	Right_knee_angle_x_PostClusterKnee	Right_knee_angle_x_PostClusterKnee SD	Right_knee_angle_x_Anatomical_3DOF	Right_knee_angle_x_Anatomical_3DOF SD	Right_knee_angle_x_AntClusterKnee_3DOF	Right_knee_angle_x_AntClusterKnee_3DOF SD	Right_knee_angle_x_Cluster4_3DOF	Right_knee_angle_x_Cluster4_3DOF SD	Right_knee_angle_x_PostClusterKnee_3DOF	Right_knee_angle_x_PostClusterKnee_3DOF SD
Right_knee_angle_x_Anatomical			2.15	1.51	3.48	1.71	1.61	0.62	1.65	0.97	1.72	1.15	3.17	1.66	1.97	2.25
Right_knee_angle_x_AntClusterKnee	1.000	0.00			3.64	1.61	1.88	1.88	2.51	1.22	2.23	0.85	3.70	0.94	2.54	1.17
Right_knee_angle_x_Cluster4	1.000	0.00	1.00	0.00			3.77	1.97	3.60	1.09	3.22	0.97	2.91	1.06	3.26	0.93
Right_knee_angle_x_PostClusterKnee	1.000	0.00	1.00	0.00	1.00	0.00			2.64	0.93	2.62	1.27	4.19	1.42	2.98	2.07
Right_knee_angle_x_Anatomical_3DOF	1.000	0.00	1.00	0.00	1.00	0.00	1.00	0.00			1.14	0.56	2.65	0.95	1.32	1.26
Right_knee_angle_x_AntClusterKnee_3DOF	1.000	0.00	1.00	0.00	1.00	0.00	1.00	0.00	1.00	0.00			2.17	0.90	1.02	1.08
Right_knee_angle_x_Cluster4_3DOF	1.00	0.00	1.00	0.00	1.00	0.00	1.00	0.00	1.00	0.00	1.00	0.00			2.06	0.65
PostClusterKnee 3DOF	1.000	0.00	1.00	0.00	1.00	0.00	1.00	0.00	1.00	0.00	1.00	0.00	1.00	0.00		

Appendix 2: Frontal plane results for RMSE between all eight marker sets in the upper section of table and cross-correlation values in the lower section of table. For each trial, RMSE and cross-correlation values were calculated for each combination comparison between two of the eight marker sets. Values were first averaged over the three repeated trials within the participants. Finally, the group mean (N=10) values and standard deviations were calculated over these individual means, which are presented in this table.

	Right_knee_angle_y_Anatomical	Right_knee_angle_y_Anatomical SD	Right_knee_angle_y_AntClusterKnee	Right_knee_angle_y_AntClusterKnee SD	Right_knee_angle_y_Cluster4	Right_knee_angle_y_Cluster4 SD	Right_knee_angle_y_PostClusterKnee	Right_knee_angle_y_PostClusterKnee SD	Right_knee_angle_y_Anatomical_3DOF	Right_knee_angle_y_Anatomical_3DOF SD	Right_knee_angle_y_AntClusterKnee_3DOF	Right_knee_angle_y_AntClusterKnee_3DOF SD	Right_knee_angle_y_Cluster4_3DOF	Right_knee_angle_y_Cluster4_3DOF SD	Right_knee_angle_y_PostClusterKnee_3DOF	Right_knee_angle_y_PostClusterKnee_3DOF SD
Right_knee_angle_y_Anatomical			1.82	0.72	2.48	1.47	2.54	0.90	2.40	1.46	2.92	0.97	5.55	2.90	4.02	1.71
Right_knee_angle_y_AntClusterKnee	0.64	0.33			3.02	1.89	1.30	0.93	3.09	1.34	2.60	1.41	5.72	2.93	3.48	1.41
Right_knee_angle_y_Cluster4	0.58	0.32	0.69	0.30			3.82	1.76	4.06	1.29	4.09	2.30	5.96	4.44	5.35	2.92
Right_knee_angle_y_PostClusterKnee	0.57	0.34	0.92	0.09	0.64	0.33			3.75	2.08	3.20	1.93	6.39	2.77	3.03	1.37
Right_knee_angle_y_Anatomical_3DOF	0.71	0.28	0.33	0.30	0.38	0.32	0.32	0.35			2.88	1.15	5.96	2.47	4.40	2.39
Right_knee_angle_y_AntClusterKnee_3DOF	0.67	0.34	0.58	0.31	0.58	0.31	0.54	0.33	0.58	0.37			5.38	2.14	2.98	2.62
Right_knee_angle_y_Cluster4_3DOF	0.52	0.32	0.49	0.37	0.57	0.30	0.42	0.36	0.49	0.29	0.51	0.33			5.95	2.37
PostClusterKnee 3DOF	0.54	0.33	0.59	0.26	0.63	0.27	0.63	0.29	0.43	0.39	0.66	0.31	0.55	0.32		

Appendix 3: Transverse plane results for RMSE between all eight marker sets in the upper section of table and cross-correlation values in the lower section of table. For each trial, RMSE and cross-correlation values were calculated for each combination comparison between two of the eight marker sets. Values were first averaged over the three repeated trials within the participants. Finally, the group mean (N=10) values and standard deviations were calculated over these individual means, which are presented in this table.

728

	Right_knee_angle_z_Anatomical	Right_knee_angle_z_Anatomical SD	Right_knee_angle_z_AntClusterKnee	Right_knee_angle_z_AntClusterKnee SD	Right_knee_angle_z_Cluster4	Right_knee_angle_z_Cluster4 SD	Right_knee_angle_z_PostClusterKnee	Right_knee_angle_z_PostClusterKnee SD	Right_knee_angle_z_Anatomical_3DOF	Right_knee_angle_z_Anatomical_3DOF SD	Right_knee_angle_z_AntClusterKnee_3DOF	Right_knee_angle_z_AntClusterKnee_3DOF SD	Right_knee_angle_z_Cluster4_3DOF	Right_knee_angle_z_Cluster4_3DOF SD	Right_knee_angle_z_PostClusterKnee_3DOF	Right_knee_angle_z_PostClusterKnee_3DOF SD
Right_knee_angle_z_Anatomical			2.39	1.08	4.62	2.28	3.10	1.18	3.40	2.12	2.93	1.35	5.53	1.79	2.65	1.09
Right_knee_angle_z_AntClusterKnee	0.87	0.12			6.64	2.02	1.33	0.56	4.21	1.59	3.76	1.16	7.34	1.99	3.80	1.60
Right_knee_angle_z_Cluster4	0.72	0.19	0.79	0.19			7.27	1.29	6.27	4.10	4.96	3.33	4.11	1.75	4.15	2.75
Right_knee_angle_z_PostClusterKnee	0.83	0.13	0.92	0.08	0.80	0.19			4.94	1.45	4.74	1.19	7.97	2.66	4.48	1.43
Right_knee_angle_z_Anatomical_3DOF	0.70	0.28	0.62	0.31	0.49	0.33	0.61	0.37			3.61	2.52	6.30	3.09	3.76	3.34
Right_knee_angle_z_AntClusterKnee_3DOF	0.73	0.20	0.72	0.25	0.60	0.29	0.68	0.31	0.76	0.23			4.96	1.54	2.75	2.02
Right_knee_angle_z_Cluster4_3DOF	0.62	0.21	0.65	0.22	0.58	0.29	0.65	0.31	0.71	0.25	0.71	0.25			4.81	2.03
PostClusterKnee 3DOF	0.72	0.25	0.72	0.24	0.71	0.23	0.77	0.26	0.59	0.38	0.70	0.31	0.58	0.38		